Purification and Physical−Chemical Properties of Methanobactin: A Chalkophore from *Methylosinus trichosporium* OB3b†

Hyung J. Kim,‡,§ Nadezhda Galeva,|| Cynthia K. Larive,⊥,@ Michail Alterman,*,|| and David W. Graham*,‡

Department of Civil, Environmental, and Architectural Engineering, University of Kansas, Lawrence, Kansas 66045, Mass Spectrometry Laboratory, University of Kansas, Lawrence, Kansas 66045, and Department of Chemistry, University of Kansas, Lawrence, Kansas 66045

Received December 15, 2004; Revised Manuscript Received February 1, 2005

ABSTRACT: Methanobactin is an extracellular, copper-binding chromopeptide from the methane-oxidizing bacterium, *Methylosinus trichosporium* OB3b, believed to be involved in copper detoxification, sequestration, and uptake. Although small (1217.2 Da), methanobactin possesses a complex three-dimensional macrocyclic structure with several unusual moieties. The molecule binds one copper and has the *N*-2-isopropylester-(4-thionyl-5-hydroxyimidazolate)-Gly^1-Ser^2-Cys^3-Tyr^4-pyrrolidine-(4-hydroxy-5-thionylimidazolate)-Ser^5-Cys^6-Met^7 sequence [Kim, H. J., et al. (2004) *Science 305*, 1612−1615]. We report methods for purifying methanobactin from *M. trichosporium* OB3b and present initial evidence of its physiological function. MALDI-TOF MS was used to systematically monitor samples for optimizing purification conditions, and for detecting and analyzing specific metal−methanobactin complexes. Purification was performed by first stabilizing the extracted compound with copper followed by separation using reversed-phase HPLC in neutral pH buffers. Purified methanobactin exhibited UV−visible maxima at 342 nm, a shoulder at 388 nm, and a broad peak at 282 nm. These features were lost upon $CuCl_2$ titration with appearance of new features at 335, 356, 290, and 255 nm. Furthermore, methanobactin contains two fluorescent moieties, which exhibit broad emissions at 440−460 nm (λ_{max}^{ex} at 388 nm) and 390−430 nm (λ_{max}^{ex} = 342 nm), respectively. Finally, methanobactin eliminates the growth lag in *M. trichosporium* OB3b and substantially increases growth rates when cultures are exposed to elevated copper levels.

Methanotrophic bacteria play a central role in the reduction of atmosphere-bound methane, eliminating as much as 80−90% of this potent greenhouse gas from aquatic, marine, and terrestrial sources (*1*, *2*). These organisms oxidize methane to methanol via a methane monooxygenase (MMO), which is the first enzyme in their catabolic pathway. Some methanotrophs possess two distinct MMOs, with the iron-containing soluble MMO (sMMO)[1] being expressed at low copper-to-biomass levels and the copper-containing particulate MMO (pMMO) being expressed at high copper-to-biomass levels (*3*, *4*). A unique trait of these organisms is their tolerance and requirement for high copper ion concentrations (a potentially toxic redox-active metal). In addition to regulating the expression of the two MMOs, increasing copper ion concentrations in the growth medium results in increases in pMMO specific activity as well as increases in the development of intracytoplasmic membranes where pMMO is found (*5*−*7*). To facilitate the uptake and delivery of adequate levels of copper, some methanotrophs such as *Methylosinus trichosporium* OB3b and *Methylococcus capsulatus* (Bath) possess a specialized copper trafficking mechanism that involves the use of a small, water soluble, chromopeptide called methanobactin for extracellular copper sequestration and subsequent transport into the cells.

The presence of methanobactin (reported earlier as CBC or CBL) from spent media of methane-oxidizing bacteria has been established for a number of years. Its presence was first implied by Fitch et al. (*8*) during the characterization of *M. trichosporium* OB3b copper uptake mutants that constitutively express sMMO in the presence of copper. The presence of the suspected copper-complexing agent(s) was confirmed by Zahn and DiSpirito (*9*) during the isolation of pMMO from *M. capsulatus* (Bath). Progress in the area of detailed structural determination has been difficult, primarily due to the uniqueness of the compound and difficulty in obtaining preparations that were pure, homogeneous, and stable. For example, Téllez et al. (*10*) isolated copper-containing ligands (CBL) of ∼500 Da from the spent media

† This work was supported by National Science Foundation Grant BES-9407286 (D.W.G.) and University of Kansas Research Development Funds (D.W.G., C.K.L., and M.A.).

* To whom correspondence should be addressed. E-mail: dwgraham@ku.edu. Phone: (785) 864-2945. Fax: (785) 864-5631. Technical issues can also be directed to M.A. at malterman@ku.edu.

‡ Department of Civil, Environmental, and Architectural Engineering.

§ Current address: Department of Biochemistry, Molecular Biology and Biophysics, University of Minnesota, Minneapolis, MN 55455.

|| Mass Spectrometry Laboratory.

⊥ Department of Chemistry.

@ Current address: Department of Chemistry, University of California, Riverside, CA 92521.

[1] Abbreviations: sMMO, soluble methane monooxygenase; pMMO, particulate methane monooxygenase; CBC, copper-binding compound; CBL, copper-binding ligand; NMS, nitrate mineral salts; MALDI-TOF, matrix-assisted laser desorption ionization time-of-flight; MS, mass spectrometry; OD, optical density; CHCA, α-cyano-4-hydroxycinnamic acid; *p*-NA, *p*-nitroaniline.

10.1021/bi047367r CCC: $30.25
Published on Web 03/10/2005

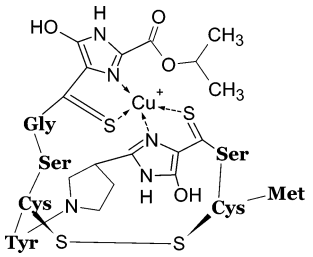

FIGURE 1: Schematic drawing of methanobactin (*12*).

of *M. trichosporium* OB3b using size exclusion high-performance liquid chromatography; however, its purity was never established. DiSpirito et al. (*11*) isolated CBCs with masses of 1218 and 779 Da (presumably similar to CBLs) also from *M. trichosporium* OB3b cultures. These compounds were purified using gel filtration chromatography, but mixtures of compounds were always found that are now suspected to have been breakdown products of a primary molecule.

Recently, the crystal structure of methanobactin from *M. trichsporium* OB3b was determined (*12*), which has confirmed early assessments that the molecule was new and complex in structure (see Figure 1). The 1.1 Å crystal structure revealed that methanobactin was indeed a chromopeptide containing a mononuclear copper center with the overall structure *N*-2-isopropylester-(4-thionyl-5-hydroxyimidazolate)-Gly^1-Ser^2-Cys^3-Tyr^4-pyrrolidine-(4-thionyl-5-hydroxyimidazolate)-Ser^5-Cys^6-Met^7 with the empirical formula $C_{45}N_{12}O_{14}H_{62}Cu$ (MW = 1217.2 Da). The two cysteines are disulfide-bridged, creating a macrocyclic structure. The chelating groups that bind copper are the N^{ϵ} atoms of the two 4-thionyl-5-hydroxyimidazolates and two S atoms of the thionyl substituents comprising a tetrahedral N,S-bidentate ligand system. The chelating moiety, as well as the pyrrolidine, exhibits unusual features in biological systems. Methanobactin has a broad structural resemblance to the iron-binding siderophores in terms of its chromopeptidic moiety and appears to have similar functions (i.e., acquisition of extracellular copper and subsequent delivery into cells; a "chalkophore", chalko = copper), although the breadth of its role relative to cell physiology and the MMO system have not been fully determined.

In this paper, we describe the isolation and purification of methanobactin that led to pure, homogeneous, and stable preparations suitable for crystallization. Protocols relied upon improved separation chemistry and MALDI-TOF MS, which produced high-quality methanobactin product thus allowing a more detailed examination of methanobactin and its metal complexes. We also report UV−vis and fluorescence spectra, characterize spectral changes upon copper binding, and present evidence on how methanobactin enhances growth and reduces toxic lags in *M. trichosporium* OB3b cultures grown under elevated copper conditions.

MATERIALS AND METHODS

Organisms and Culture Conditions. *M. trichosporium* OB3b cells were cultured in a 2.5 L bioreactor controlled by a Bioflo 3000 controller (New Brunswick) containing 2 L of copper-deficient nitrate minimal salts (NMS) medium. The reactor was sparged with instrument-grade methane at 25 mL/min. Air was supplied and regulated to maintain soluble O_2 levels at 30% saturation, previously determined to provide optimal growth rates (*13*). The cultures were grown in batch mode to early to midexponential phase specified by optical density measurements at 600 nm ($0.4 < OD_{600} < 0.6$) prior to harvesting for methanobactin. Typically, 1.5 L of the culture was harvested and replaced with the same volume of NMS medium. The culture was regrown to an OD_{600} between 0.4 and 0.6 before reharvesting.

Isolation and Purification of Methanobactin. The general isolation procedure was a modified version of the protocol developed by DiSpirito et al. (*11*). For each harvest, the spent medium was centrifuged at 9000*g* for 20 min to pellet cells. The supernatant was filtered through 0.2 μm membrane filters and loaded onto C_{18} solid-phase extraction (SPE) Sep-Pak cartridges (Waters Associates). The bound material was washed with reagent-grade Milli-Q water and eluted with either an 80% acetonitrile (ACN)/0.1% trifluoroacetic acid (TFA) solution or 60% ACN without TFA. The eluant was lyophilized for concentration and storage.

After extraction, methanobactin was purified by reversed-phase HPLC. The lyophilized extract was dissolved in Milli-Q water and purified using reverse-phase chromatography on a semipreparative Vydac 218 TP1010 column (10 mm × 250 mm, 300 Å). Chromatography was performed using a Summit HPLC system (Dionex) equipped with multiwavelength UV−vis detector. The HPLC separation was performed at a flow rate of 3 mL/min. The mobile phase was composed of 10 mM ammonium or sodium acetate at pH 6.5 (solution A), and acetonitrile with 10 mM ammonium or sodium acetate (solution B) (80:20, v/v). The column was equilibrated with 20% solution B and then the gradient profile was changed to 40% solution B over the course of 20 min and then to 100% solution B over the course of 2 min. Absorbance was monitored at 392 and 345 nm, and the major fractions were collected manually, lyophilized, and analyzed using MALDI-TOF MS. Fractions that contained the molecular ion of interest were rechromatographed on a Vydac 218TP52 (C_{18}) reverse-phase analytical HPLC column (2.1 mm × 250 mm, 300 Å).

MALDI-TOF Mass Spectral Analysis. MALDI mass spectra were obtained on a Voyager-DE STR MALDI TOF mass spectrometer (Applied Biosystems) in both positive and negative reflector modes. The acquisition mass range was typically 500−1500 Da. The matrix solutions used were α-cyano-4-hydroxycinnamic acid (CHCA) in a 50% ACN/0.1% TFA solution (10 mg/mL) or *p*-nitroaniline (*p*-NA) [35 mM in a 4:1 mixture of water and ethanol (pH 6.5)]. Typically, 1 μL of a 5 mg/mL solution of methanobactin was diluted 1:10 with either α-cyano-4-hydroxycinnamic acid (CHCA) or *p*-nitroaniline matrix. For some experiments, peptide solutions were desalted and concentrated using ZipTip C_{18} pipet tips (Millipore) prior to analysis.

Amino Acid Analysis and Partial HCl Hydrolysis. Methanobactin was completely hydrolyzed at 105 °C for 20 h with constant boiling in 6 N HCl (Pierce Endogen) in the vapor phase with 0.1% (w/v) phenol and 1% (w/v) 2-mercaptoethanol under a N_2 atmosphere. Phenol and 2-mercaptoethanol were added to prevent halogenation of tyrosine and oxidation of methionine, respectively. The sample vials were evacuated and flushed with N_2 several times using a Waters Pico-Tag Workstation. After hydrolysis, the samples were derivatized using a final solution of ethanol, water, triethy-

lamine, and phenyl isothiocyanate (7:1:1:1, v/v) for 90 min. The hydrolysate was analyzed on a Beckman Gold HPLC System with an Inertsil 5 μm ODS-2 250 mm × 3.0 mm column (MetaChem Technologies, Lake Forest, CA). For partial hydrolysis, 10% (1.2 N) HCl in the vapor phase at 95 °C was used and the progress of the reaction monitored using MALDI-TOF MS analysis.

UV−Vis and Fluorescence Spectroscopy. UV−vis absorbance measurements were taken using a dual-beam Shimadzu UV160U spectrophotometer. Intrinsic fluorescence measurements were performed using a Photon Technology International (PTI) QuantaMaster luminescence spectrofluorometer. For luminescence measurements, UV−vis absorbance maxima were used as initial excitation wavelengths to scan for corresponding maximum emission wavelengths. The acquired maximum emission wavelength was then used to scan for more accurate excitation wavelengths. Slits were 4 nm for excitation and emission.

Copper and pH Titration. Metal-free methanobactin was prepared by extensive dialysis against EDTA and subsequent Sep-Pak extraction and lyophilization. Copper addition was carried out by incremental addition of $CuCl_2$ (0.5 μM additions) to 50 μM methanobactin dissolved in 20 mM sodium phosphate buffer (pH 6.5). After each addition, the sample was allowed to equilibrate for 5 min in the dark before the UV−vis absorbance spectra were recorded. Experience had indicated that stable spectra typically developed in less than 30 s, although 5 min was selected because it provided very reproducible results. A similar system was used for measuring changes in fluorescence as a function of copper addition. For pH titration experiments, the pH of the solution was decreased in 0.5−1 pH unit increments by the addition of trace metal grade HCl that had been prepared at concentrations of either 3, 1, or 0.5 N, and the UV absorption spectra were recorded after each pH change. Titrations were performed using a flow-through pH meter and reference microelectrode system (Microelectrodes, Inc., Bedford, NH).

Metal Analysis. Determinations of the amount of Cu, Zn, Ni, and Fe ions complexed to methanobactin were made using a Perkin-Elmer Analyst 300 atomic absorption spectrometer equipped with a graphite furnace. Prior to analysis, 1−2 mg of purified methanobactin was digested in 2 mL of 80% trace metal grade HNO_3 for 2−3 h at 90 °C until the solution turned colorless. All standards and blanks were prepared using 2% HNO_3 in reagent-grade Milli-Q water. Glassware was soaked overnight in 50% HNO_3. Reported values are averages of at least triplicate measurements.

Biological Activity of Methanobactin. To assess the influence of purified methanobactin on growth and toxicity reduction in *M. trichosporium* OB3b, different proportional ratios of 10.0 μM copper and HPLC-purified methanobactin were provided to a series of 50 mL cultures grown on copper-limited NMS medium in 165 mL serum vials crimp-sealed with Tygon stoppers. The experiment was initiated by the addition of an "overnight" culture grown under copper-limited conditions to the test vials at a starting OD of 0.05. Copper and methanobactin were then provided at ratios ranging from 10:1 to 0.58:1 to triplicate vials, and the following parameters were monitored: length of lag phase, maximal growth rate, doubling time, maximal OD reached, time required to reach the maximal OD, and the OD after 72 h. A 50:50 (v/v) mixture of methane and air (60 mL total) was injected daily throughout the experiment by syringe, and cultures were agitated on a shaker table at 120 rpm. The OD was measured every 10−12 h until the stationary phase.

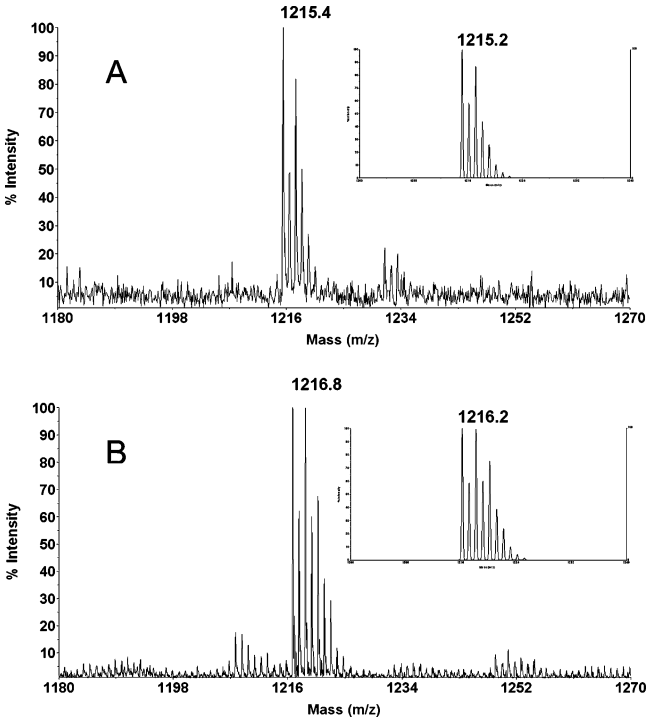

FIGURE 2: Negative ion, reflector mode MALDI-TOF mass spectra of methanobactin complexed with (A) copper (*m*/*z* 1215.4) and (B) Zn (*m*/*z* 1216.8) as revealed by the isotopic distribution of the isotopes at natural abundances. The insets show the expected isotopic distribution of methanobactin ($C_{44}H_{57}N_{12}O_{15}S_5$) complexed with (A) Cu or (B) Zn.

RESULTS

Isolation and Detection of the Metal−Methanobactin Complex Using MALDI-MS. To maximize methanobactin production, *M. trichosporium* OB3b cells were grown in copper-deficient media expressing sMMO. Under this condition, typical yields, involving relatively short culture residence times (~3 days with a culture OD_{600} of ~0.7), were ~15−20 mg/L of spent medium. Longer residence times (~5 days) increased the yield, but also considerably increased the amounts of degradation products. Therefore, the optimal time for harvest, in terms of highest yield with low levels of degradation products, was determined to be during mid to late exponential phases of growth.

MALDI-TOF MS analysis of methanobactin isolated from late exponential-phase cultures indicates a molecular ion at *m*/*z* 1153 $[M - H]^-$ and an ion at *m*/*z* 1215 $[M - 2H + {}^{63}Cu^+]^-$ for the corresponding copper complex, even though no supplemental copper was added to the media (*12*). The difference of *m*/*z* 62 between the copper-free and copper-complexed ligand indicates a stoichiometry of 1:1. The presence of copper was indicated by the relative intensity of the peak at *m*/*z* 1217 (Figure 2A) attributed to $[M - 2H + {}^{65}Cu^+]$. Some preparations also contained Zn as evidenced by the isotopic distribution observed for the ion at *m*/*z* 1217 (Figure 2B) and later confirmed by atomic adsorption metal analysis (data not shown). However, Zn-complexed methanobactin was observed only when contaminating copper concentrations in the growth media were less than ~0.06

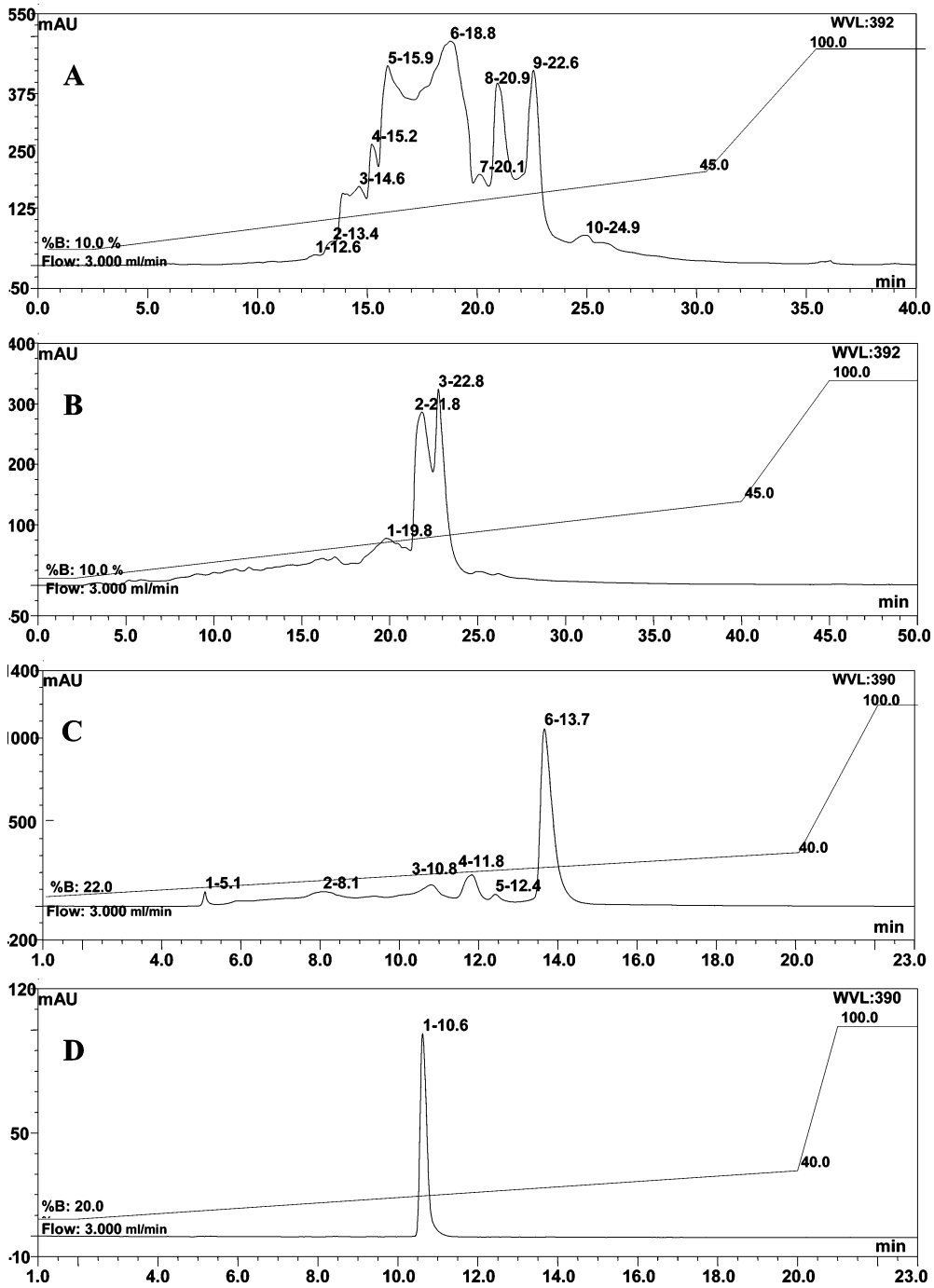

FIGURE 3: Comparison of HPLC spectra under different conditions for methanobactin: (A) using a 0.1% TFA/ACN (pH 2) gradient, (B) using a 10 mM NaAc/ACN (pH 6.5) gradient, (C) after optimization using a 10 mM NaAc/ACN (pH 6.5) gradient, copper-stabilized, and (D) purity check of the major fraction from condition C.

μM (determined by amino acid analysis). This provides a qualitative illustration of methanobactin's specificity for copper even though other divalent metals ions such as Zn were present at much higher levels (2 μM).

RP-HPLC Purification at Acidic and at Near-Neutral pH's. Initial reverse-phase C_{18} HPLC purification of methanobactin involved mobile phases typically used for the separation of peptides (0.1% TFA at pH 2 and 80% acetonitrile with 0.1% TFA). The elution profile in Figure 3A is representative of chromatography under this condition. Broad peaks and poor resolution were typical. Usually, four to five major fractions were observed, and all fractions were heterogeneous as revealed by MALDI-TOF MS analysis. All fractions contained the molecular species of interest at *m*/*z* 1239 $(M - 2H + Cu + Na)^+$. However, various unidentified ions at *m*/*z* 1147, 1115, 1165, and 974 were also observed in high abundance (result not shown). Attempts to further purify each fraction by repeated chromatography were not successful as each peak refractionated.

After a series of separation trials, the HPLC procedure was modified to use near-neutral buffers (pH 6−6.5) that produced better results than separations utilizing acidic buffers. Optimal conditions were achieved when TFA was omitted and either 10 mM ammonium acetate (pH 6.5) or sodium acetate (pH 6.5) was used for mobile phase A and 80% ACN was used for mobile phase B. Two major yellow,

fluorescent fractions were observed using this strategy (Figure 3B). MALDI-TOF analyses of these two peaks showed that the major ion present was *m*/*z* 1238 $(M - H + Cu + Na)^+$. Fraction 1 also contained the ion at *m*/*z* 1215 $(M + Cu)^+$, while fraction 3 contained *m*/*z* 1216 $(M + H + Cu)^+$ and *m*/*z* 1260 $(M + H + Cu + 2Na)^+$.

Chromatography was further improved by saturating the harvested medium with an ~1000-fold molar excess copper to exchange other bound divalent metals before purification. The insoluble copper was removed by centrifugation. The resulting product was highly pure and stable (Figure 3C). Analytical rechromatography of the major peak (even after storage for 5 days) showed minimal breakdown when the samples were stored at 4 °C in the dark (Figure 3D). After lyophilization, the purified product was reddish-brown as opposed to the yellow color exhibited by samples purified without copper stabilization. Crystallization of purified methanobactin (in a 40:60 water/methanol mixture) was achieved using vapor diffusion with ethyl acetate as the precipitating agent (*12*, *14*), resulting in reddish-brown needle-shaped crystals (see Figure S1 of the Supporting Information).

Influence of Matrices in MALDI Analysis of Methanobactin. Initial MALDI-TOF mass spectral analyses were performed in linear mode using CHCA, which is a preferred matrix for peptides but is strongly acidic (pH <2). Interestingly, CHCA did not produce useable methanobactin spectra in positive linear and reflector modes. Changes in peptide and protein conformations and, in many cases, denaturation are often induced by strongly acidic conditions. This was especially pertinent to methanobactin because of its observed instability in acidic solutions as indicated by HPLC purification experiments. Therefore, a *p*-nitroaniline matrix solution at pH 6.5 was examined for its suitability as a matrix (*15*). Use of *p*-NA greatly improved the ionization of methanobactin and allowed measurements in positive and negative mode reflector modes, resulting in greater mass accuracy and resolution. Furthermore, the isotopic peaks related to the metal ions of interest were consistently fully resolved with this matrix, allowing the unambiguous determination of the presence or absence of the complexed metal.

Amino Acid Composition and End Group Identification. Amino acid analysis yielded 2 moles of glycine, 2 moles of cysteine, and 1 mole each of serine, methionine, tyrosine, and proline. In reference to the crystal structure (*12*), we now know that methanobactin contains only 1 mol of glycine. Furthermore, the pyrrolidine present in the crystal structure was likely detected as a proline because of its structural resemblance. Amino acid analysis also showed the presence of 1−2 mol of unknown moieties that eluted immediately before proline in the reversed-phase HPLC separation.

Edman degradation of purified methanobactin failed, suggesting that the N-terminus was blocked. The blocking group could be removed using mild HCl hydrolysis (1.2 N HCl, 95 °C) for 15 min. MALDI-TOF MS analysis of the hydrolysate revealed that the N-terminus was protected by a function with a mass of 43 units, which was tentatively assigned to cleavage of an *N*-acetyl group (CH_3CO^-). We now know, however, that the loss is due to cleavage across the ester bond with an isopropyloxy leaving group in addition to hydration (*12*, *14*) (Figure 4A). Extended hydrolysis analyzed up to 24 h resulted in further cleavage of the backbone. However, it was difficult to arrive at unambiguous sequence assignments prior to crystal structure determination. Limited proteolysis (ladder sequencing) yielded unambiguous C-terminal information where proteinase K, Pronase, and carboxypeptidase Y all released methionine (*m*/*z* 1217−131) within 15 min (Figure 4B). Further digestion of the peptide backbone, however, could not be achieved even after incubation for 48 h.

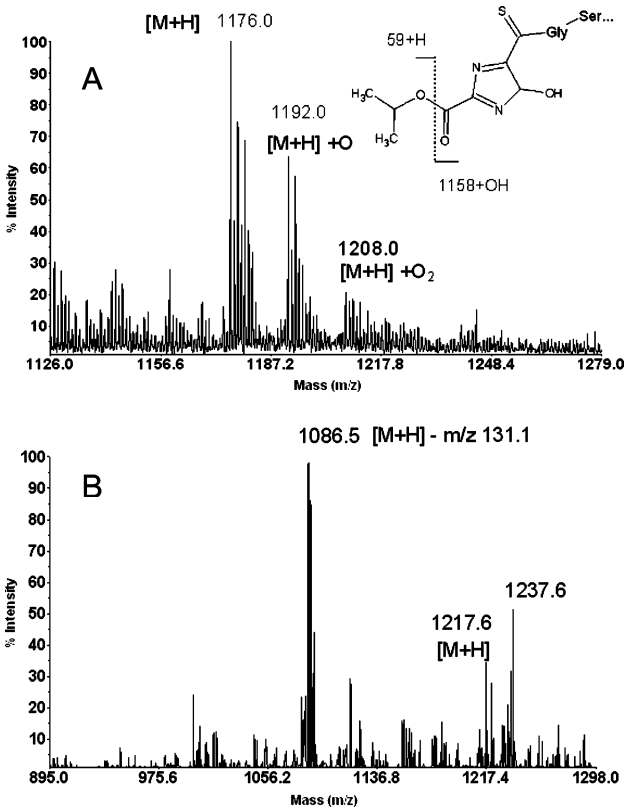

FIGURE 4: End group analysis of methanobactin. (A) Product of mild gas-phase HCl hydrolysis (1.2 N, 95 °C). The *m*/*z* at 1176.0 is a result of cleavage across the ester bond with subsequent hydration (inset). Peaks at *m*/*z* 1192.0 and 1208.0 are oxygen adducts of the peak at *m*/*z* 1176.0. (B). Product of overnight proteinase K digestion as a result of hydrolysis of the C-terminal methionine residue.

UV−Vis Spectrum. As isolated, methanobactin possessed an absorption maximum at 342 nm, a shoulder at 388 nm, and somewhat featureless absorption in the 240−280 nm range (Figure 5A). There were no spectral features beyond 400 nm, and the addition of dithionite did not change the observed spectra (*14*). When methanobactin was dialyzed against EDTA at pH 2, a conversion of the shoulder at 388 nm to a peak was observed (Figure 5B). Exposure of the methanobactin solution to UV light decreased the absorbance at 388 nm, which strongly suggests that this chromophoric function is photosensitive. Extended exposure eliminates the peak altogether. It is likely that the absorbance in the 281 nm region is due to the aromatic side chain of tyrosine which has a λ_{max} of 274 nm. Thus, the peaks at 388 and 342 nm are due most likely to the two hydroxy thionyl imidazolates that coordinate the copper in a distorted tetrahedral geometry (*12*), where the presence of the carbonyl substituent on one of the two chromophores leads to two distinct absorbance maxima.

To probe copper binding to methanobactin, absorbance spectra were measured after each successive addition of

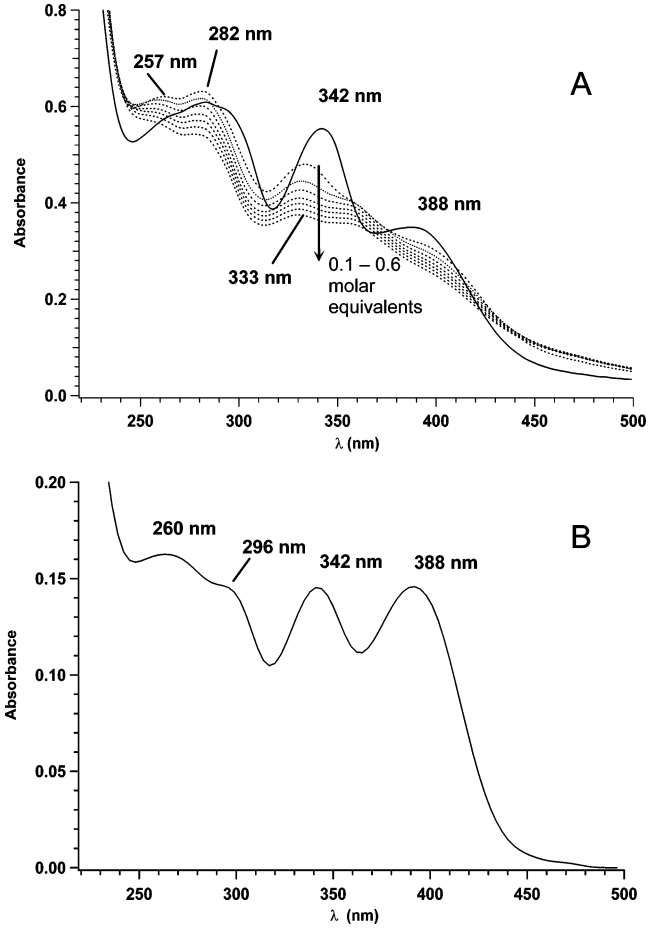

FIGURE 5: UV−vis absorption spectra of methanobactin. (A) Methanobactin as isolated (—) and upon sucessive copper (as $CuCl_2$) additions from 0.1 to 0.6 molar equiv (•••). (B) Methanobactin after extensive dialysis against EDTA. Note the more intense peak at 388 nm relative to the peak at 342 nm when compared to the "as isolated" spectrum.

$CuCl_2$ (0.1 molar equiv) (Figure 5A). After the first addition of $CuCl_2$, the three characteristic peaks at 388, 342, and 281 nm were lost with appearance of new features at 335, 290, and 255 nm. The most notable difference was the decrease in the intensity of the 388 nm peak. Further, copper addition eliminated spectral features altogether around this region. Cystine possesses an inflection point at ~250 nm. As such, the inflection point at 255 nm is probably due to the disulfide-linked cysteine residue, suggesting that copper binding mediates linkage of the two cysteinyl sulfurs. Further increasing the copper concentration increased the absorbance at 255 nm relative to the 335 nm peak. When methanobactin is saturated with copper, as is the case when methanobactin is copper stabilized before purification, the 330−360 nm region is resolved into two peaks at 333 and 356 nm.

The pH dependence of the absorption spectra was investigated by pH titration from pH 9 to ~1. From pH 9 to 4.9, no changes were observed in the spectral features between 330 and 360 nm (Figure 6). Below pH 5, the peak at 356 nm was gradually lost relative to the peak at 333 nm until at pH 1.2 the spectrum in the 356 nm region resembled that of metal-free methanobactin, suggesting a loss of copper. Additionally, an ~5% dilution occurred through the titration, although this effect is small compared with the absolute changes in absorption as the pH was reduced.

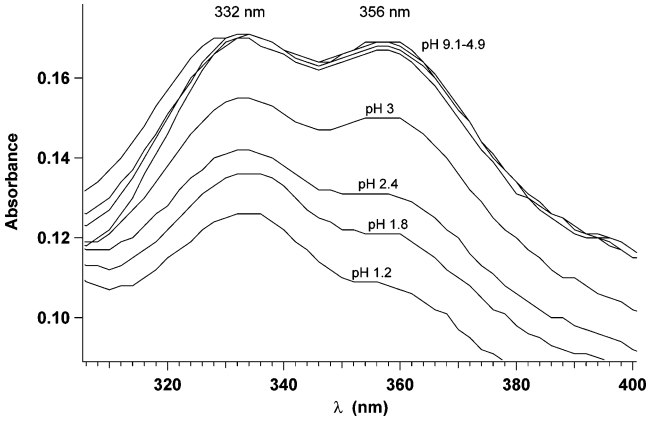

FIGURE 6: Effect of pH on the absorption spectra of methanobactin showing the relative decrease in the peak at ~356 nm to the peak at 332 nm.

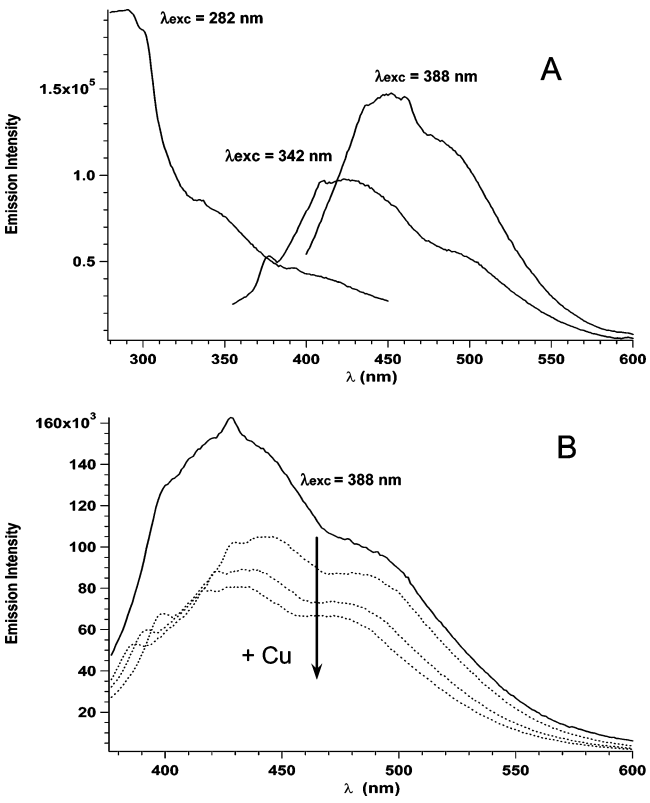

FIGURE 7: (A) Emission spectra of as isolated methanobactin in water (25 °C) when excited using the wavelength indicated above each spectrum. (B) Effect of addition of copper ($CuCl_2$) on fluorescence emission spectra for methanobactin isolated from the spent media.

Fluorescence. Purified methanobactin displayed three distinct emission bands (Figure 7A) when excited at wavelengths of 282, 342, and 388 nm. The most intense band occurred at ~280 nm (λ_{ex} = 282 nm) and was attributed to the emission of tyrosine, which has a λ_{max} at 275 nm when excited at 260 nm (*16*). This band also possessed the most distinct peak shape. Tyrosine is one of few molecules with an excitation maximum wavelength at or near its emission maximum wavelength. The other two emission bands were broad and featureless. Their overall intensities were low, consistent with the low luminescence exhibited by methanobactin. The emission around 390−430 nm, corresponding

Table 1: Effects of Purified Methanobactin on Various Growth Parameters on *M. trichosporium* OB3b in NMS Medium Containing 10 μM Copper[a]

	0 mg of MBn, 10:0 Cu:MBn	0.1 mg of MBn, 7:1 Cu:MBn	0.3 mg of MBn, 2.3:1 Cu:MBn	0.5 mg of MBn, 1.38:1 Cu:MBn	0.7 mg of MBn, 1:1 Cu:MBn	0.9 mg of MBn, 0.77:1 Cu:MBn	1.2 mg of MBn, 0.58:1 Cu:MBn
lag phase (h)	70	20	10	<5	<5	<5	<5
maximal growth rate (h^{-1})	14.3×10^{-3}	15.2×10^{-3} (6%)	23.5×10^{-3} (64%)	26.6×10^{-3} (86%)	30.9×10^{-3} (116%)	35.0×10^{-3} (145%)	32.9×10^{-3} (130%)
doubling time (h^{-1})	48.5	45.6	29.5	26	22.4	19.8	21
OD_{600} max	0.3	0.29 (−3%)	0.361 (20%)	0.361 (20%)	0.411 (37%)	0.405 (35%)	0.411 (37%)
time to OD_{600} max (h)	60	100	100	75	50	50	50
OD_{600} after 72 h	0.118	0.159	0.317	0.352	0.367	0.386	0.385

[a] MBn represents methanobactin. Numbers in parentheses represent percent increases relative to cultures with no methanobactin supplementation.

to purple luminescence, contained a shoulder around 490−500 nm, and exhibited the lowest intensity. This emission corresponded to the chromophore exhibiting a λ_{max}^{abs} of 340 nm ($\lambda_{ex}^{max} = 342$ nm). Another broad emission band around 440−460 nm, corresponding to the observed blue emission, contained a shoulder around 480 nm and was detected using a λ_{max}^{ex} at 388 nm.

The fluorescence exhibited by methanobactin was rapidly quenched upon addition of $CuCl_2$ (Figure 7B). The tyrosine emission was quenched by more than 70% within 10 s of the first 0.1 molar equiv copper addition (result not shown). Quenching was more gradual in the 342 and 388 nm emission bands where the first addition of copper decreased emission by ~13 and ~35%, respectively. Further additions of $CuCl_2$ decreased emission intensities more dramatically. Iron-binding fluorescent siderophores have been found to exhibit similar properties upon binding to iron ions (*17*).

Biological Activity. Methanobactin was hypothesized, in this and in previous works, to be an agent for copper sequestration and uptake, copper detoxification, and a possible growth promoter in pMMO-bearing organisms, including *M. trichosporium* (*7*−*11*). Therefore, the biological activity of purified methanobactin was assessed by providing methanobactin at different Cu:methanobactin ratios to *M. trichosporium* OB3b cultures grown under copper-limited conditions that were rapidly shifted to high copper concentrations (10.0 μM Cu). The experiment assessed (1) whether methanobactin suppressed the "copper-shock" lag commonly observed in *M. trichosporium* OB3b upon sudden exposure to elevated copper and (2) whether the growth rate increased as a function of methanobactin level at higher copper levels.

The following growth parameters were analyzed: length of lag phase, maximal growth rate, doubling time, maximal OD_{600} reached, time required to reach the maximal OD_{600}, and the OD_{600} after 72 h (Table 1). As expected, cultures that were switched from copper-limited conditions to 10.0 μM Cu without methanobactin exhibited very extended growth lags; however, the lags were progressively shortened as the Cu:methanobactin supply ratio approached 1:1. For example, growth lag was reduced from 70 to <5 h as more methanobactin was provided. Methanobactin addition also stimulated growth as indicated by increased growth rates and "net" OD levels. Observed increases reached maximal values at methanobactin:Cu ratios of ~1.0, which is consistent with the presumed copper-to-methanobactin binding stoichiometry.

DISCUSSION

Methanobactin is a unique and structurally complex molecule. The presence of multiple, unusual non-amino acid moieties, including a pyrrolidine and thionyl imidazolates, together with the fact that a tetrapeptide (Gly-Ser-Cys-Tyr) comprises the longest peptidic chain, suggests that methanobactin is nonribosomally synthesized. In fact, recent genomic analysis of *M. capsulatus* (BATH) indicates the presence of putative nonribosomal peptide synthetase (NRPS) sequences, including components of adenylation and thiolation domains of a synthetase, which suggest the possibility of a NRPS system for methanobactin and/or siderophores in this organism (*18*). Such a mechanism is possible for methanobactin in *M. trichosporium* OB3b and is a key topic for investigation.

In this work, we have produced methanobactin of a purity suitable for crystal growth. The observation that purified methanobactin stimulates growth and decreases lags in cultures "shocked" with 10 μM copper is a good indication that the biological activity was retained in the isolated compound after purification. We have also shown that *M. trichosporium* OB3b produces a single molecular species with a mass of 1217 Da containing copper. However, under acidic purification conditions, methanobactin seems to become unstable probably because of the release of the metal ion as suggested by pH-dependent absorption features at 388 nm.

This observation has many important implications. For example, this phenomenon likely explains the mixtures that were observed in previous isolations (*11*). The components, designated CBC-L_1 ($M_r = 1218$ Da) and CBC-L_2 ($M_r = 779$ Da), had been presumed to be different forms of methanobactin. However, it now appears that CBC-L_2 was an artifact of the low-pH conditions used for isolation. The siderophore azotobactin is also unstable in solution, especially at acidic pH's (*19*, *20*), and displays similar behavior during purification. For example, during growth at neutral pH, *Azotobacter vinelandii* produces one form of the siderophore called azotobactin D. However, during purification under acidic conditions, another form is observed (azotobactin δ). Further, the destabilizing effects of low pH are weakened when the siderophores have iron bound.

Methanobactin can be isolated under copper-deficient conditions, and using cells expressing sMMO. This indicates that some level of the molecule is produced by *M. trichosporium* independent of pMMO expression, although the

detailed relationship between MMO expression, extracellular copper levels, and methanobactin production is currently unknown. Some hints, however, have been provided in this and in previous works. The work here shows that the presence of methanobactin in the growth medium dramatically stimulates growth, which strengthens the notion that the compound either enhances copper uptake, reduces toxicity, or both. Further, the effects are strongly linked to the Cu:methanobactin molar ratio, with saturation effects occurring when the ratio was approximately 1.0. These observed growth effects might be related to increased pMMO activities in cultures supplemented with methanobactin (*7*) leading to the supposition that (1) pMMO activity in vivo could be limited by intracellular copper ion concentrations, (2) methanobactin might act to increase the availability of copper ions by sequestration and uptake, and (3) the compound appears to play a key role in decreasing copper toxicity as indicted by reduced growth lags in cultures amended with methanobactin.

Further, DiSpirito et al. noted that methanobactin levels in the spent media were highest when cells were expressing pMMO and starved for copper at sMMO−pMMO switchover, which suggests that its production may be linked to pMMO expression and function (*10*). This notion is further strengthened by the fact that methanobactin has been found to be associated with the pMMO enzyme complex in *M. capsulatus* (Bath) (*8*) and in the washed membrane fraction of *M. trichosporium* OB3b (*10*), although methanobactin may not be intrinsically incorporated into the pMMO. Results from a recent active preparation of pMMO from *M. capsulatus* (Bath) suggest that of the 8−10 copper atoms associated with the enzyme, 6−10 are found complexed to methanobactin (*6*). The most probable role of methanobactin, when taking into account all accumulated evidence, is that it is used by the organism to sequester copper from the extracellular environment, rather than relying on simple diffusion or ion channels to acquire copper which can involve much slower kinetics. However, its specific role once in the membrane is still unknown.

One of the more interesting aspects of methanobactin is that the complexed copper appears to be present in the Cu(I) oxidation state as suggested by electron paramagnetic resonance analysis on partially purified methanobactin (*9*) and determined by X-ray photoelectron spectral analysis on purified methanobactin (*12*). The UV−vis spectrum of methanobactin provides a further indication of copper's oxidation state. Blue copper proteins (type I copper proteins) exhibit a strong absorption around 600 nm, which is derived from a sulfur-to-copper charge transfer transition with the copper in the oxidized Cu(II) state (*21*, *22*). However, UV−vis spectral features of metallothioneins, which typically bind copper as Cu(I), generally appear in the 230−400 nm range as the metal binds to the thiolate groups (*23*). The absence of absorption features above 400 nm suggests that the thionyl sulfurs of methanobactin act as the reducing ligands. The addition of the reducing agent sodium dithionite also did not change the spectral features of methanobactin, which further suggests a stable Cu(I) oxidation state once copper is incorporated into the molecule.

The presence of methanobactin in methanotrophic bacteria has several fundamental implications in and beyond methanotrophs, especially since information related to copper physiology is broadly lacking in biological systems (including copper sequestration, uptake, and distribution). However, methods presented here, which are highly effective at purifying molecules such as methanobactin, should substantially aid in broader studies of related compounds in other methanotrophs and unknown copper-related compounds in other systems. Specific to *M. trichosporium* OB3b, now that the detailed structure of methanobactin has been resolved, molecular mechanisms of copper homeostasis and trafficking can be pursued, including the possible function of methanobactin in relation to pMMO.

ACKNOWLEDGMENT

We thank Dima Yakovlev (University of Kansas Biochemical Research Services Lab) and Todd Williams (University of Kansas Molecular Structures Group Mass Spectrometry Lab) for invaluable technical assistance and use of instruments, and Laura Lucas for NMR analysis. We also thank Alan Hooper, Ed Solomon, and Ray Carter for discussions; and Brad Elmore for discussions and review of the manuscript.

SUPPORTING INFORMATION AVAILABLE

A 1000-fold magnified image of crystals used to develop the crystal structure for methanobactin is provided. This material is available free of charge via the Internet at http://pubs.acs.org.

REFERENCES

1. Hanson, R. S. (1980) Ecology and diversity of methylotrophic bacteria, *Adv. Appl. Microbiol. 26*, 3−39.
2. Reeburgh, W. S. (1996) "Soft Spots" in the Global Methane Budget, in *Microbial Growth on C1 Compounds* (Lidstrom, M. E., and Tabita, R. F., Eds.) pp 334−342, Kluwer Academic Press, London.
3. Stanley, S. H., Prior, S. D., Leak, D. J., and Dalton, H. (1983) Copper stress underlies the fundamental change in intracellular location of methane monooxygenase in methane- oxidising organisms: Studies in batch and continuous cultures, *Biotechnol. Lett. 5*, 487−492.
4. Murrell, J. C., McDonald, I. R., and Gilbert, B. (2000) Regulation of expression of methane monooxygenases by copper ions, *Trends Microbiol. 8*, 221−225.
5. Prior, S. D., and Dalton, H. (1985) The effect of copper ions on membrane content and methane monooxygenase activity in methanol-grown cells of *Methylococcus capsulatus* (Bath), *J. Gen. Microbiol. 131*, 155−163.
6. Scott, D. B. J., and Higgins, I. J. (1991) The effect of growth conditions on intracytoplasmic membranes and methane monooxygenase activities in *Methylosinus trichosporium* OB3b, *J. Gen. Microbiol. 125*, 63−72.
7. Choi, D. W., Kunz, R. C., Boyd, E. S., Semrau, J. D., Antholine, W. E., Han, J. I., Zahn, J. A., Boyd, J. M., de la Mora, A. M., and DiSpirito, A. A. (2003) The membrane-associated methane monooxygenase (pMMO) and pMMO-NADH:quinone oxidoreductase complex from *Methylococcus capsulatus* (Bath), *J. Bacteriol. 185*, 5755−5764.
8. Fitch, M. W., Graham, D. W., Arnold, R. G., Agarwal, S. K., Phelps, P., and Georgiou, G. (1993) Phenotypic characterization of copper-resistant mutants of *Methylosinus trichosporium* OB3b, *Appl. Environ. Microbiol. 59,* 2771−2776.
9. Zahn, J. A., and Dispirito, A. A. (1996) The membrane-associated methane monooxygenase from *Methyloccus capaulatus* (Bath), *J. Bacteriol. 178*, 1018−1029.
10. Téllez, C. M., Gaus, K. P., Graham, D. W., Arnold, R. G., and Guzman, R. Z. (1998) Isolation of copper biochelates from *Methylosinus trichosporium* OB3b and soluble methane monooxygenase mutants, *Appl. Environ. Microbiol. 64*, 1115−1122.

11. Dispirito, A. A., Zahn, J. A., Graham, D. W., Kim, H. J., Larive, C. K., Derrick, T. S., Cox, C. D., and Taylor, A. (1998) Copper-binding compounds from *Methylosinus trichosporium* OB3b, *J. Bacteriol. 180*, 3606−3613.
12. Kim, H. J., Graham, D. W., DiSpirito, A. A., Alterman, M. A., Galeva, N., Larive, C. K., Asunskis, D., and Sherwood, P. M. (2004) Methanobactin, a copper-acquisition compound from methane-oxidizing bacteria, *Science 305*, 1612−1615.
13. Kim, H. J., and Graham, D. W. (2001) Effect of oxygen level on simultaneous nitrogenase and sMMO expression and activity in *Methylosinus trichosporium* OB3b and its sMMO^{C} mutant, PP319: Aerotolerant N2 fixation in PP319, *FEMS Microbiol. Lett. 201*, 133−138.
14. Kim, H. J. (2003) Isolation, structural determination, and characterization of a novel copper-binding compound from *Methylosinus trichosporium* OB3b, Ph.D. Dissertation, University of Kansas, Lawrence, KS.
15. Salih, B., Masselon, C., and Zenobi, R. (1998) Matrix-assisted laser desorption/ionization mass spectrometry of noncovalent protein-transition metal ion complexes, *J. Mass. Spectrom. 33*, 994−1002.
16. Longworth, J. W. (1971) in *Excited States of Proteins and Nucleic Acids* (Steiner, R. F., and Weinryb, I., Eds.) MacMillan, London.
17. Xiao, R., and Kisaalita, W. S. (1998) Fluorescent pseudomonad pyoverdines bind and oxidize ferrous ion, *Appl. Environ. Microbiol. 64*, 1472−1476.
18. Ward, N., Larsen, E., Sakwa, J., Bruseth, L., Khouri, H., Durkin, A. S., Dimitrov, G., Jiang, L., Scanlan, D., Kang, K. H., Lewis, M., Nelson, K. E., Methe, B., Wu, M., Heidelberg, J. F., Paulsen, I. T., Fouts, D., Ravel, J., Tettelin, H., Ren, Q., Read, T., DeBoy, R. T., Seshadri, R., Salzberg, S. L., Jensen, H. B., Birkeland, N. K., Nelson, W. C., Dodson, R. J., Grindhaug, S. H., Holt, I., Eidhammer, I., Jonasen, I., Vanaken, S., Utterback, T., Feldblyum, T. V., Fraser, C. M., Lillehaug, J. R., and Eisen, J. A. (2004) *PLoS Biol. 2*, 1616−1628.
19. Meyer, J. M., and Abdallah, M. A. (1978) The fluorescent pigment of *Pseudomonas fluorescens*: Biosynthesis, purification and physicochemical properties, *J. Gen. Microbiol. 107*, 319−328.
20. Demange, P., Bateman, A., Dell, A., and Abdallah, M. A. (1988) Structure of Azotobactin D, a siderophore of *Azotobacter vinelandii* Strain D (CCM 289), *Biochemistry 27*, 2745−2752.
21. Solomon, E. I., Baldwin, M. J., and Lowery, M. D. (1992) Electronic structures of active sites in copper proteins: Contributions to reactivity, *Chem. Rev. 92*, 521−542.
22. Pierloot, K., De Kerpel, J., Ryde, U., and Roos, B. O. (1997) Theoretical study of the electronic spectrum of plastocyanin, *J. Am. Chem. Soc. 119*, 218−226.
23. Stillman, M. J. (1992) Metallothionein, in *Synthesis, structure, and properties of metallothioneins, phytochelatins, and metal−thiolate complexes* (Stillman, M. J., Shaw, C. F., and Suzuki, K. T., Eds.) VCH Publishers, New York.

BI047367R